

# Structure and Methods in the Field of Technical Logistics

**Georg Kartnig**

Professor  
Vienna University of Technology  
Faculty of Mechanical Engineering  
Institute for Engineering Design and  
Logistics Engineering

*The discipline of Technical Logistics deals with material handling on three levels: 1. Components of material handling; 2. Conveyors; and 3. Logistics systems. The subjects of these three levels can be investigated with three methods: 1. Analytical calculation; 2. Simulation; and 3. Testing. The following paper uses three case studies to describe how problems in the area of Technical Logistics can be solved with the help of current technologies.*

**Keywords:** FEM, multi body simulation, queuing theory, logistics simulation.

## 1. INTRODUCTION

The Institute for Engineering Design and Logistics Engineering at the Vienna University of Technology engages in research into material handling and logistics engineering at three levels:

- Material handling (e.g. wire ropes, belts and chains);
- Conveyors (e.g. cranes, belt conveyors and AS-RS);
- Logistics systems (e.g. distribution centres, warehouses and container terminals).

Different methodologies can and should be used to investigate each level, namely:

- Analytical calculation; and/or
- Simulation; and/or
- Testing of actual equipment.

This leads to a three by three matrix (Table 1), and everyone working in the field of logistics engineering should be familiar with all nine cells of this matrix.

**Table 1. Structure and methods of logistics engineering**

	Analytical calculation	Simulation	Testing
Logistics systems	Queuing theory	Logistics simulation	Measurement of cycle times
Conveyors	Mechanics	FEM, MBS	Measurement of $F, M, a, v, \omega, \sigma, \epsilon, \dots$
Components of material handling	Mechanics	FEM, MBS	Tension test, test stands

Each of the three methods has its particular advantages and disadvantages:

- **Analytical calculation:**  
Advantages: deep understanding of coherences, fast and easy variation of parameters;  
Disadvantages: error-prone;
- **Simulation:**  
Advantages: descriptive, fail-safe;  
Disadvantages: long calculation times;

- **Testing of actual equipment:**

Advantages: close to reality;

Disadvantages: time-consuming.

In most of the cases it makes sense to use at least two methods to solve a problem in order to obtain reliable results. The benefits of doing so will be shown in the following three case studies. Each case study can be allocated to one of the aforementioned levels of material handling.

## 2. CASE STUDY 1: ANALYTICAL AND EXPERIMENTAL INVESTIGATIONS OF A SELF RESCUE SYSTEM

Rescue devices are designed to enable people to rope down out of dangerous situations (e.g. out of burning buildings) and in this way bring themselves to safety. Besides professional rescue devices like those used by firemen, military personnel and the police, there has been a tendency in the past few years to design models for private users.

Our Institute received such a rescue device for investigation and improvement to verify that it could pass a mandatory standard examination (DIN EN341 [1]).

Like most rescue devices this one is also based on the fly-wheel brake principle. It contains two fly-wheel brakes of the simplex-drum brake type [2]. The two drum brakes are synchronised with gears. A rope wheel is rigidly connected to one of these gears. A rope is placed around this rope wheel, on which rescue overalls can be fixed on each end with the help of carabiners (Fig. 1).

For the roping down process the rescue device is attached to a window frame or to the ceiling above the balcony. The person wanting to rope down puts on a rescue overall, then fixes it to one end of the rope and abseils along the wall of the building. Arriving on the ground floor, he/she takes off the rescue overall. Now the other end of the rope is situated at the level the first person evacuated from, so that a second person with a rescue overall can escape in the same manner.

The most important characteristic of these rescue devices is their reliability under any imaginable conditions.

The DIN EN341 standard defines the specifications and test processes for rescue devices. Among other parameters this standard defines the descent speed for descending persons weighing 30 kg, 75 kg and 150 kg as being between 0.5 m/s and 2.0 m/s.

Received: October 2009, Accepted: November 2009

Correspondence to: Dr Georg Kartnig  
Faculty of Mechanical Engineering,  
Getreidemarkt 9/E307, 1060 Vienna, Austria  
E-mail: georg.kartnig@tuwien.ac.at

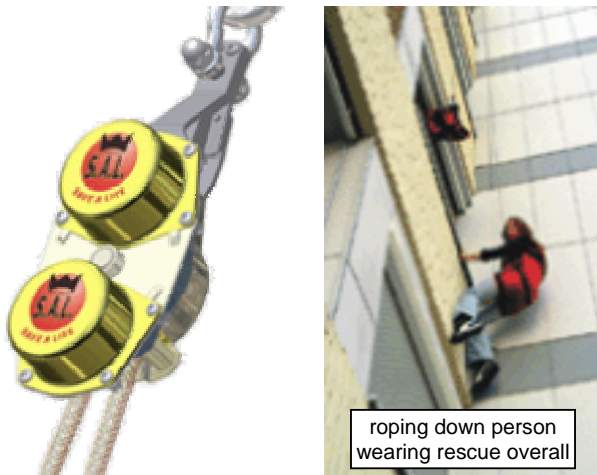


Figure 1. Rescue device

Experimental tests at our institute were carried out in accordance with this standard. In addition the temperature of the drum brakes was investigated, so as to be able to make a clear pronouncement about the durability of the brake linings used.

To reach a deeper understanding of the functioning of the rescue device, the inter-relationship between the descent speed, descent weight and friction coefficient of the brake linings was investigated using the calculation outlined in the following section.

## 2.1 Analytical calculation

As mentioned above, the function of the rescue device is based upon the principle of fly-wheel brakes. Figure 2 shows the construction of the drum brake and Figure 3 the calculation model with the acting forces that form the basis for the calculation [3].

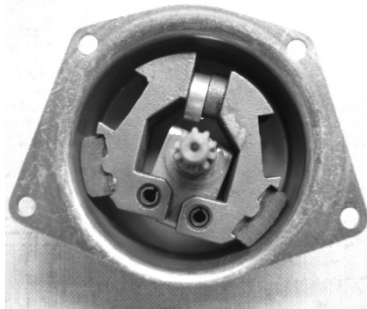


Figure 2. Fly-wheel brake

The centrifugal force on the left, pulled brake arm is:

$$F_{f,le} = m_{le} r_{le} \dot{\xi}^2 \quad (1)$$

Here  $m_{le}$  is the mass of the left brake arm,  $r_{le}$  the distance between the rotation axis and the centre of gravity of the brake arm, and  $\dot{\xi}$  the angular velocity of the rotating brake.

Out of the momentum equilibrium around point A, one derives for the left brake arm (with  $l_2$  and  $l_3$  equal for left and right brake arm):

$$F_{f,le} l_{7,le} - F_{r,le} l_3 - F_{n,le} l_2 = 0 \quad (2)$$

where

$$F_{r,le} = \mu F_{n,le} \quad (3)$$

the friction force  $F_{r,le}$  for the pulled brake arm can be derived following the simple Coulomb friction model:

$$F_{r,le} = \frac{\mu F_{f,le} l_{7,le}}{\mu l_3 + l_2} \quad (4)$$

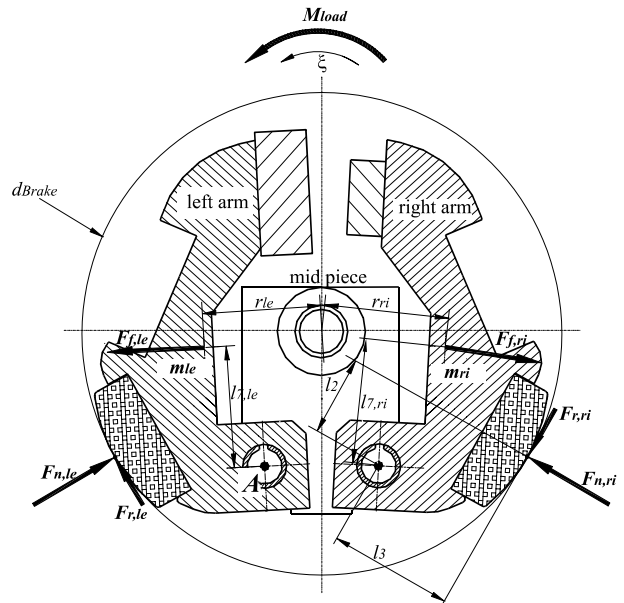


Figure 3. Forces on the fly-wheel brake (static model)

For the other – the pushed – brake arm the sign of the denominator must be inverted. So  $F_{r,ri}$  becomes:

$$F_{r,ri} = \frac{\mu F_{f,ri} l_{7,ri}}{-\mu l_3 + l_2} \quad (5)$$

and the brake force  $F_{\text{Brake}}$  of one drum brake becomes:

$$F_{\text{Brake}} = F_{r,le} + F_{r,ri} \quad (6)$$

As our rescue device consists of two drum brakes, the complete brake force  $F_{\text{Brake,tot}}$  is:

$$F_{\text{Brake,tot}} = 2F_{\text{Brake}} \quad (7)$$

and the total brake momentum:

$$M_{\text{Brake,tot}} = F_{\text{Brake,tot}} \frac{d_{\text{Brake}}}{2} i_{\text{Gear}} \quad (8)$$

with  $d_{\text{Brake}}$  as the inner diameter of the drum brake and  $i_{\text{Gear}}$  as the gear ratio between the rotating brake arms and the rope wheel.

This total brake momentum  $M_{\text{Brake,tot}}$  is equal to the pulling force on the rope of the rescue device (= weight force of a descending person) multiplied by the effective radius of the rope wheel  $r_{\text{rope-wheel}}$ :

$$M_{\text{Brake,tot}} = m_{\text{Person}} g r_{\text{rope-wheel}} \quad (9)$$

This enables the angular velocity of the rotating brake arms  $\dot{\xi}$  to be calculated for the stationary operation.

$$\dot{\xi} = \sqrt{\frac{m_{\text{Person}} g \frac{d_{\text{Rope}}}{2} i_{\text{Gear}}}{d_{\text{Brake}} \mu \left( \frac{m_{le} r_{le} l_{7,le}}{\mu l_3 + l_2} + \frac{m_{ri} r_{ri} l_{7,ri}}{-\mu l_3 + l_2} \right)}} \quad (10)$$

The descent speed  $v_{\text{Rope}}$  depending on the weight of the descending person and the friction coefficient  $\mu$  can also be obtained:

$$v_{\text{Rope}} = \frac{\dot{\zeta} r_{\text{rope-wheel}}}{i_{\text{Gear}}} \quad (11)$$

Figure 4 shows the descent speed as a function of the friction coefficient  $\mu$ . One can see that – with a given weight of the brake arms – the friction coefficient  $\mu$  must be between 0.07 and 0.2, so that the descent speed of 30 kg, 75 kg and 150 kg lies within the prescribed range of between 0.5 m/s and 2 m/s.

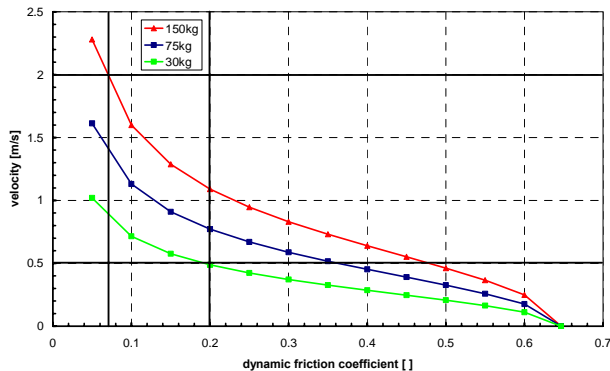


Figure 4. Descent speed

## 2.2 Simulation

As the static calculation does not consider variable forces and the changing geometry caused by rotation, it cannot describe the system completely. Furthermore the descending person is hanging on a vibratory visco-elastic rope. The following section goes on to describe all these phenomena.

For the dynamic modelling there are some more forces involved than for the static calculation. These are mainly inertia forces and the weight affect dynamic relations with dependence on rotation angle  $\zeta$ .

Figure 5 shows all the geometric relations and acting forces. ADAMS MBD software was used for modelling.

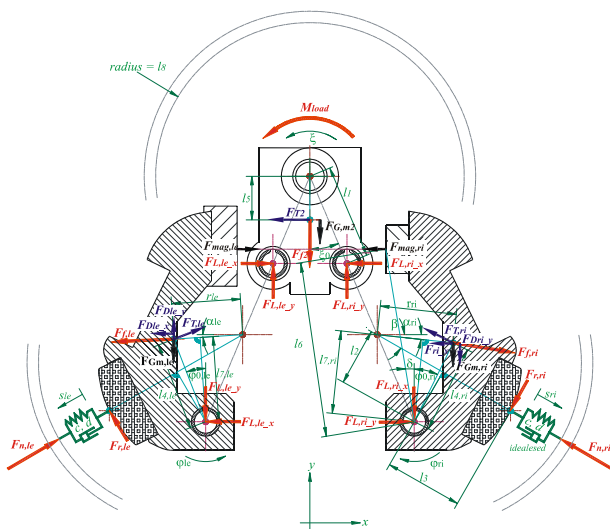


Figure 5. Forces and geometries – dynamic modelling

Figure 6 shows one result of the dynamic simulation: the deformation of the brake drum by the left (pulled)

and right (pushed) brake arm with  $\mu = 0.41$  given from brake linings manufacturer and a 75 kg person.

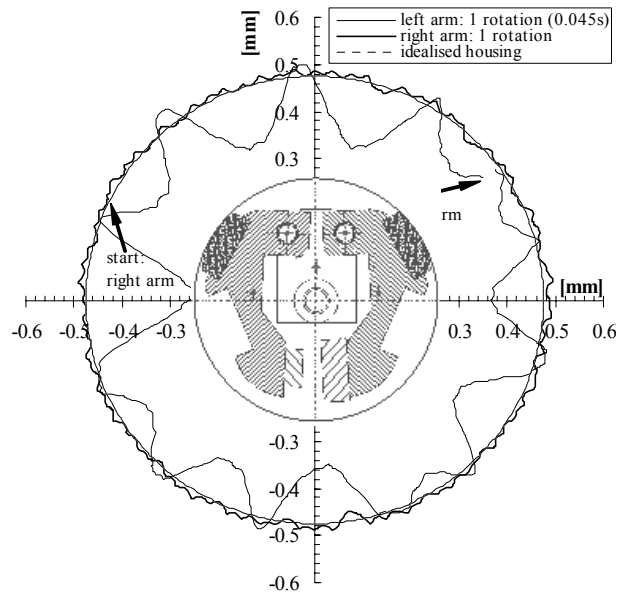


Figure 6. Penetration of brake drum during one rotation of left pulled and right pushed brake arm reduced to relative amplitudes with idealised housing radius equals 0.48 mm

There are two main frequencies for the arm oscillation:  $\sim 1770$  Hz for the right, pushed arm and  $\sim 270$  Hz for the left pulled arm. Both frequencies are very high and will not cause resonant vibrations in combination with the non-stiff rope.

Figure 7 shows a comparison of the results of the analytic calculation with the results of simulation. The curves correspond in a wide area. Differences result from two effects:

- From the twist of the middle piece and as a consequence of the shifting of the boundary points of brake linings and brake drums;
- From the fact that the boundary forces and thus the friction forces fluctuate in a wide range.

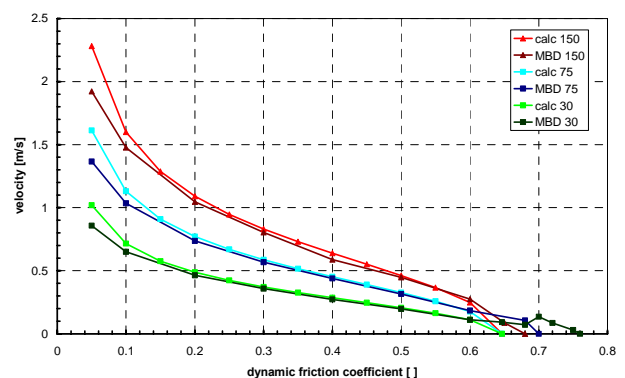


Figure 7: Comparison of analytic calculation with multi body simulation

## 2.3 Experimental investigations

To measure the real descent speed and to validate static and dynamic models, the rescue device was investigated experimentally. For this purpose, a test stand was built at our institute. It consists of a stiff frame made of aluminium profiles and plates. On one of these plates, the rescue device is fixed (Fig. 8).

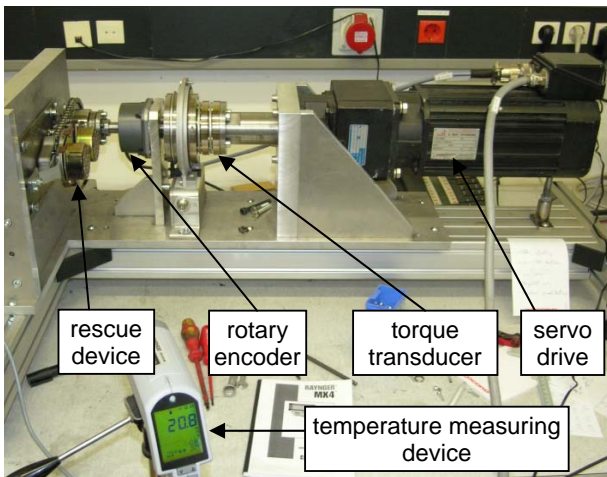


Figure 8. Rescue device test stand

In the rescue device the rope wheel was replaced by a chain wheel, so that the roping down force could be induced by a chain drive. The necessary torque is applied by a torque controlled servo drive with a flange mounted planetary gearbox.

The test stand also contained a rotary encoder to measure the descent speed and a torque measuring device to control the torque of the servo drive. In addition, a contactless working temperature measuring device was mounted on a tripod. All the measuring data were recorded with the aid of LabVIEW measuring software.

During the measurements the following data were recorded: the speed of the chain wheel, the drive torque and the temperature of the drum brake.

The measuring process was essentially equivalent to DIN EN 341 [1], with the only difference that the rescue device was tested for a descent height of 300 m instead of 100 m as prescribed in the standard.

DIN EN 341 prescribes only a descent height of 100 m. Therefore one test cycle consists of the following parts:

The rescue device is loaded with a torque corresponding to a descent weight of 75 kg. The descent height is 300 m, and afterwards there is a break of 90 s. The next part of the test – also with a descent weight of 75 kg – goes the other way round. All in all there are seven tests with a descent weight of 75 kg. After that there is one test with a descent weight of 150 kg and at the end one with a descent weight of 30 kg.

In Figure 9 one can see seven measuring curves that show the descent speed with a descent weight of 75 kg. The descent speeds lie between ~ 0.35 m/s and ~ 1.2 m/s, whereas the first descent processes show higher and the later ones slower speeds. This means that the heating of the drum brake causes an increase in the friction coefficient of the brake linings.

With the measured descent speeds and the aid of the equations mentioned above the related friction coefficients can be calculated. They lie between 0.15 and 0.48. This results – with the given brake arm weight of 47.5 g ( $m_{\text{current stage}}$ ) – in calculated descent speeds of 0.25 m/s for a descent weight of 30 kg,  $\mu = 0.48$  and 1.50 m/s for a descent weight of 150 kg,  $\mu = 0.15$ . That means the rescue device is too slow.

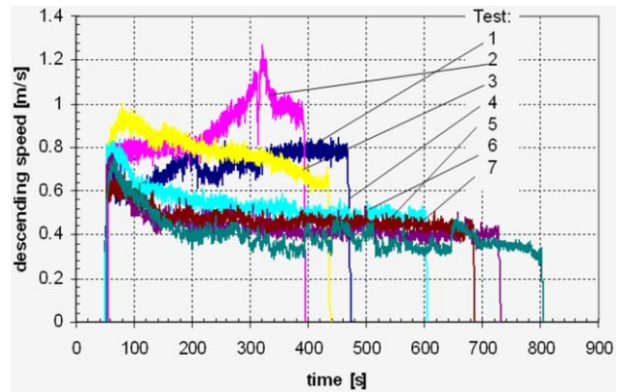


Figure 9. Results of the third test cycle

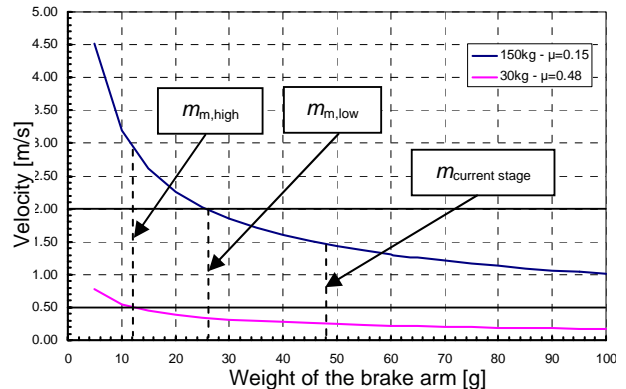


Figure 10. Connection between mass of one brake arm, dynamic friction coefficient and descent speed (field colour and limiting curves 0.5 and 2.0 m/s)

To remain – given the measured friction coefficients – within the prescribed speed range of 0.5 m/s to 2.0 m/s, the mass of the brake arms has to be reduced. Figure 10 reveals that a reduction in the weight of the brake arms is necessary so that the weight of each brake arm lies between 12 g and 26 g ( $m_{\mu,\text{high}}$  and  $m_{\mu,\text{low}}$ ). Even with these brake arm weights it is not possible to remain completely within the prescribed speed range. Either the rescue device is too fast ( $m_{\mu,\text{high}}$ , 150 kg and  $\mu_{\text{min}}$ ) or it is too slow ( $m_{\mu,\text{low}}$ , 30 kg and  $\mu_{\text{max}}$ ).

We recommend the highest possible weight of 26 g, because this way it is guaranteed that the maximum speed is not above 2.0 m/s but can be below 0.5 m/s. This lower speed will occur with 30 kg persons (children) descending. Therefore it is intended to support the descending process by applying additional hand force on the tight side rope by a person observing the rescue of children.

This brake arm weight minimises the problems with regard to brake arm design and heating.

## 2.4 Summary of case study 1

In the static calculation the connection between descent weight, the friction coefficient of the brake linings and the descent speed was shown.

With the help of the multi-body simulation could show that there are no critical situations because of resonance.

In the experimental investigation we were able to show that the real friction coefficients vary in a broad range.



Based on this knowledge, the weight of the brake arms was reduced from 47.5 to 26 g. The descending process of children has to be supported by the application of additional hand force.

### 3. CASE STUDY 2: INVESTIGATIONS OF A FRICTION DAMPER FOR STORAGE MACHINES

The second object of investigation is the damper of a storage machine.

The crash of storage machines with 70 % of their maximum speed against a damper is the highest load that can occur with these devices. Therefore it plays an important role in dimensioning them.

This crash test must be performed during the acceptance trial and there no ductile deformations in the storage machine may occur. The dampers used should thus be so designed that the kinetic energy is transformed into braking energy at minimal forces.

#### 3.1 Experimental investigations

To measure the characteristics of dampers available on the market as well as of newly developed devices, a damper test stand for storage machines was constructed at the Institute for Technical Logistics at Graz University of Technology. The test stand consists mainly of a vehicle and a structure for fixing different types of dampers (Fig. 11).

The vehicle – a truncated storage machine – consists of a chassis made of sheet metal (Fig. 12). It runs on two wheels driven by a speed-controlled DC motor.

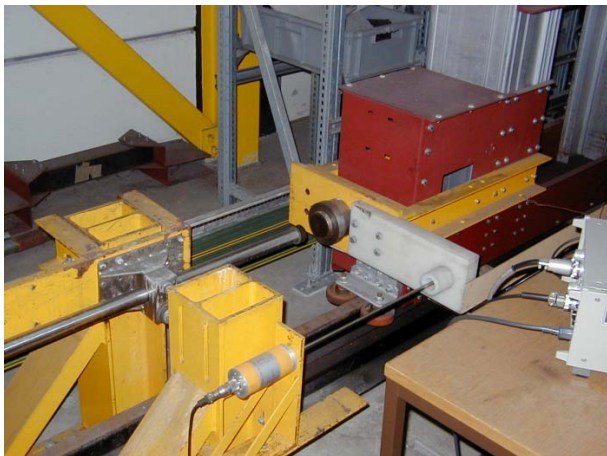


Figure 11. Damper test stand

Maximum speed is 3.2 m/s. To vary the weight of the vehicle from 700 kg to 2200 kg, it is possible to put metal plates between the two truncated beams.

Figure 13 shows the hardware for the data acquisition: for the force measurement a 200 kN load cell with an accuracy of 0.1 % is used. It is fixed to the vehicle, and data transfer to the measurement amplifier is accomplished using a trailing cable. To measure the deviation of the damper, a linear absolute displacement transducer is used.

The equipment also includes a light barrier having two purposes: it triggers the measurement short before the vehicle strikes the damper, and it switches off the DC motor of the vehicle.

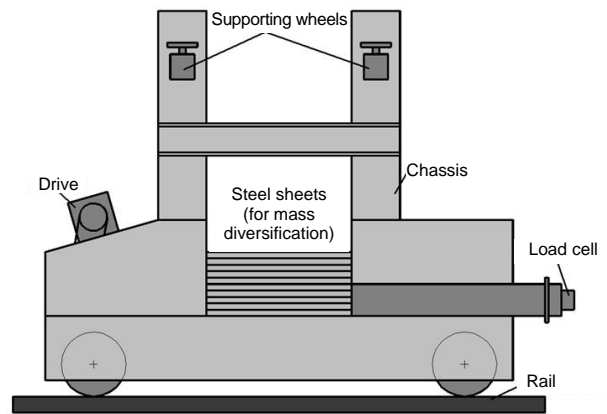


Figure 12. Vehicle of the damper test stand

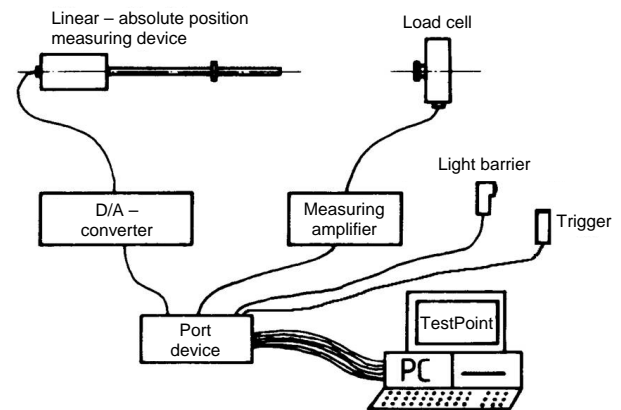


Figure 13. Hardware for the data acquisition

By measuring displacement versus time it is also possible to calculate the actual speed of the vehicle shortly before the crash. This way the kinetic energy of the crashing mass is also known.

The acquisition and analysis of the measured data is performed by a PC with appropriate software.

The damper that was investigated by our institute was a so-called friction damper, developed by TGW GmbH, an Austrian company. It consists of a rod made of steel with a rubber cap on one end. The rod is clamped between two clamp blocks with a defined clamp force of 8500 N. This is achieved by using a distance tube and disc springs which are deformed by a defined path. The friction damper and the clamp block are shown in Figures 14 and 15 [4].

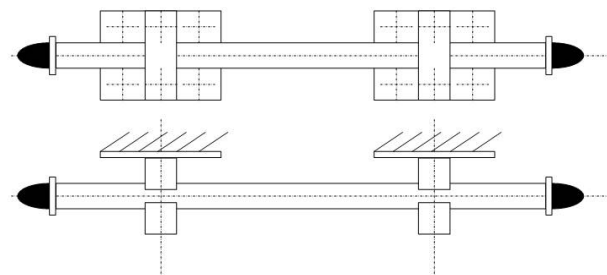


Figure 14. Friction damper

Figure 16 shows the characteristics of such a friction damper. At the left end one sees the parabolic increase of the damping force, which describes the deformation of the rubber cap. The following decrease shows the shifting of the tube in the clamp blocks. In combination with the elastic rubber cap the inert mass of the rod

forms an oscillating system. This is the reason for the wide amplitudes in the friction damper.

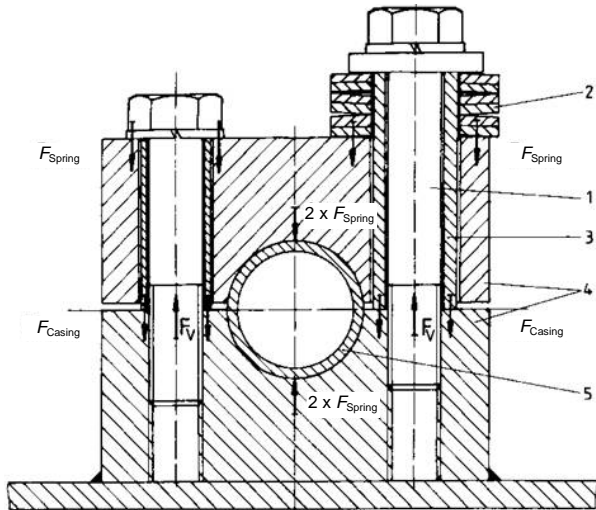


Figure 15. Clamp block

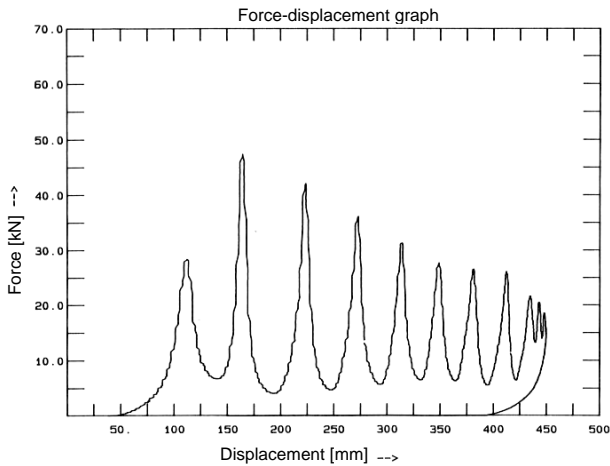


Figure 16. Characteristic of a friction damper

### 3.2 Simulation

To gain an improved understanding of the incidences during a crash as well as to optimise the friction damper by varying the relevant parameters, a simple simulation model was generated using Matlab Simulink (Fig. 17). Here  $m_1$  stands for the mass of the vehicle, and  $m_2$  for the mass of the rod of the friction damper.  $m_1$  and  $m_2$  are connected by a spring and a damper. Spring rate and damping rate correspond to the rubber cap. The rod  $m_2$  is connected to the inertial frame by the friction force  $F_{fr}$ .

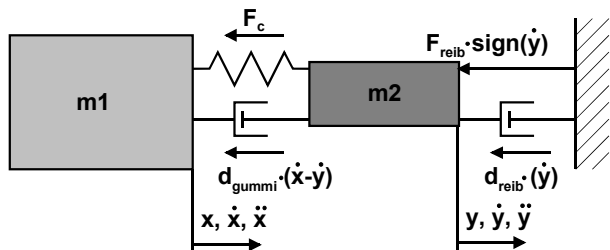


Figure 17. Simulation model of vehicle and friction damper

This simulation model can be described by two differential equations, according to the equations of motion of the vehicle  $m_1$  and the rod of the friction damper  $m_2$ .

$$-m_1 \ddot{x} - F_c - d_r (\dot{x} - \dot{y}) = 0 \quad (12)$$

$$-m_2 \ddot{y} + F_c + d_r (\dot{x} - \dot{y}) - \text{sign}(\dot{y})(F_{fr} + d_{fr} \dot{y}) = 0 \quad (13)$$

Since it includes a non-linear term, the differential equation system had to be transformed into a block diagram in Simulink (Fig. 18). This block diagram was solved by simulation with the help of MATLAB Simulink.

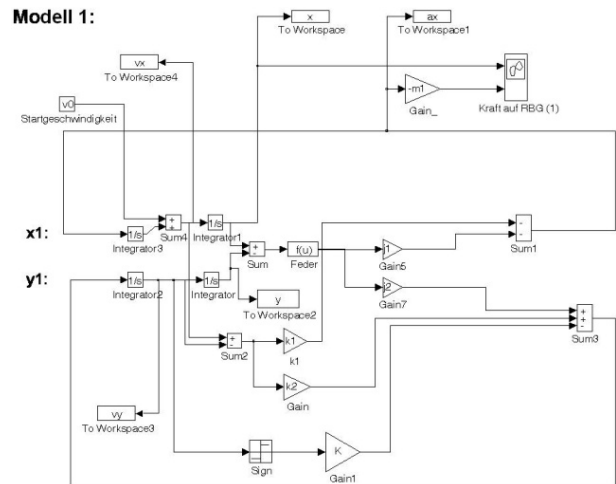


Figure 18. Block diagram

The result of the simulation is shown in Figure 19. This exhibits excellent qualitative and quantitative agreement between measurement and calculation as compared with Figure 16. The simulation model thus appears to be appropriate to detailed research into the incidences during the damper crash and to parameter studies.

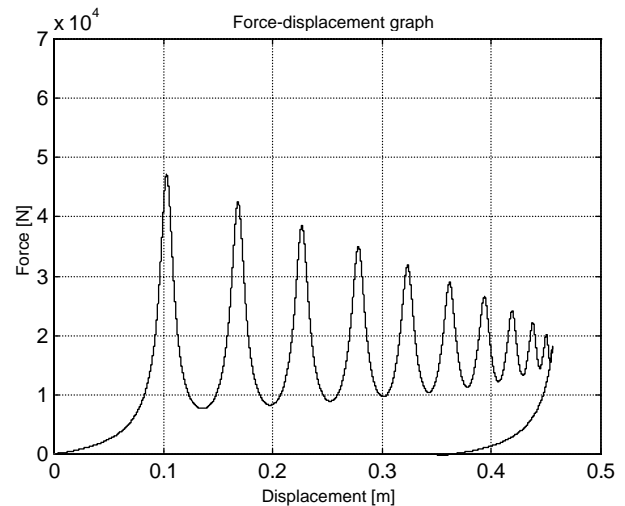


Figure 19: Result of the simulation

The characteristics of friction dampers are mainly influenced by:

- The spring rate and damping rate of the rubber cap;
- The mass of the damper rod;
- The friction force;
- The damping force in the clamp blocks.

The ideal characteristic is one where the maximum force  $F_{max}$  is as close as possible to the mean force  $F_{mean}$ . By varying the parameters mentioned above, we tried to achieve this perfection.

Fixing the friction damper to the storage machine and locating only two buffer stops at both ends of the storage rack alley has several advantages:

- Costs decrease, because only one friction damper is needed;
- Space requirements decrease;
- The load for the storage machine decreases to the friction force between damper rod and clamp blocks.

Figure 20 shows the simulation model for this configuration.

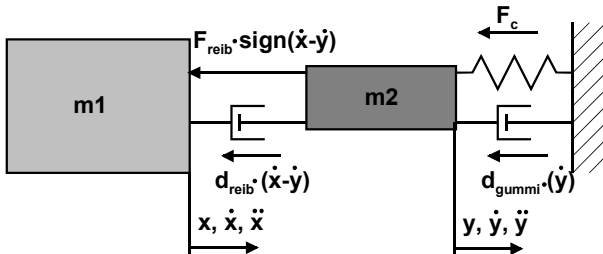


Figure 20. Simulation model of the friction damper fixed at the storage machine

It can be described with the following equations:

$$-m_1 \ddot{x} - F_c - d_r (\dot{x} - \dot{y}) = 0 \quad (14)$$

$$-m_2 \ddot{y} + F_c + d_r \dot{y} + \text{sign}(\dot{x} - \dot{y})(F_{fr} + d_{fr}(\dot{x} - \dot{y})) = 0. \quad (15)$$

This differential equation system was solved again with MATLAB Simulink. The result is shown in Figure 21. First the rubber cap is deformed again. When the load of the friction damper is high enough, the rod shifts against the clamp blocks and the load for the storage machine is limited at the height of the friction force.

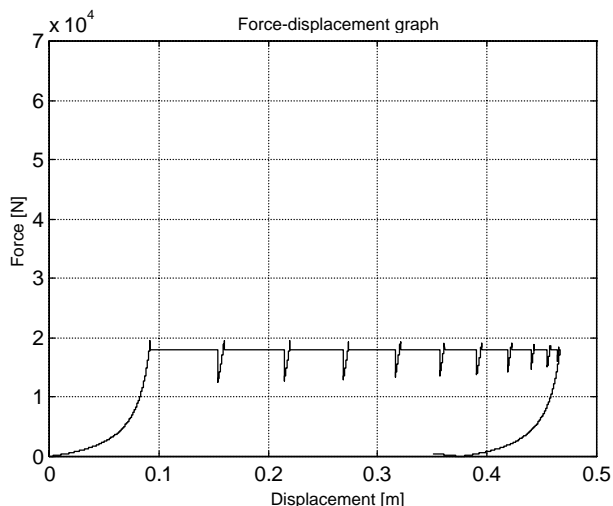


Figure 21. Result of the simulation with friction damper fixed at the storage machine

This configuration is very close to the ideal characteristics for friction dampers mentioned above. It has been in use with the TGW GmbH storage machines for several years.

### 3.3 Summary of case study 2

Friction dampers should transform the kinetic energy of vehicles into braking energy at minimal possible forces.

The braking process was investigated in detail using a combination of measurements and simulation. This enabled an optimum friction damper with minimum braking forces, attached to the vehicle, to be identified.

## 4. CASE STUDY 3: DEVELOPMENT OF AN AUTOMATED TERMINAL WITH RAIL GUIDED VEHICLES

Global distribution of goods is mainly based on container transportation. Rapid growth over the past 50 years has led to a global fleet of 15 million containers handling two-thirds of international goods transportation. Most of the terminals use manually driven reach stackers working like forklift trucks, equipped with special load lifting devices. Some terminals like that in the port of Hamburg, Germany operate with automated guided truck vehicles. Due to the high investment and operating costs such equipment is mainly appropriate for large terminals with high throughput.

The requirement here was to develop a solution for a small terminal utilising cost-effective, automated technology. The approach presented in this case study is based on industrial heavy duty material handling components and was developed at the Institute of Logistic Systems at Graz University of Technology [5].

The handling process requires loading of the empty containers with pallets and transportation of the containers to a container crane, which loads the container ship or serves a storage yard. The technical requirements are:

- Loading and transportation of 20-ft and 40-ft containers with a maximum weight of 24.000 kg and 30.480 kg, respectively;
- Required throughput: seven containers/hour;
- Four docks for container loading.

A simple and effective solution is a closed loop rail guided vehicle system, with the empty containers travelling to the loading docks on vehicles. After being filled the full containers travel to the container crane, which separates the container from the vehicle when loading the ship. The empty vehicles finally travel to the empty container loading station, where the cycle is completed.

The following section describes the system layout and operation including the technical components of the transportation system.

### 4.1 System layout and operation

The system layout in Figure 22 exhibits a triangular shape according to the available floor space. The components utilised are rail guided carriers, turntables and container cranes.

In the first section forklift trucks move empty containers on top of the rail guided vehicles. These vehicles move along the rails and with turntables to the second section providing individual docking stations. A total of four docks is sufficient to load the empty containers with paper goods on pallets or with paper coils. During the loading process the containers remain on the carriers. Thereafter the carriers move to the third section, where cranes separate the containers from the carriers, which travel back empty to the first section, where the cycle is completed. This simple arrangement

needs only five turntables next to the rail track and a number of vehicles yet to be determined.

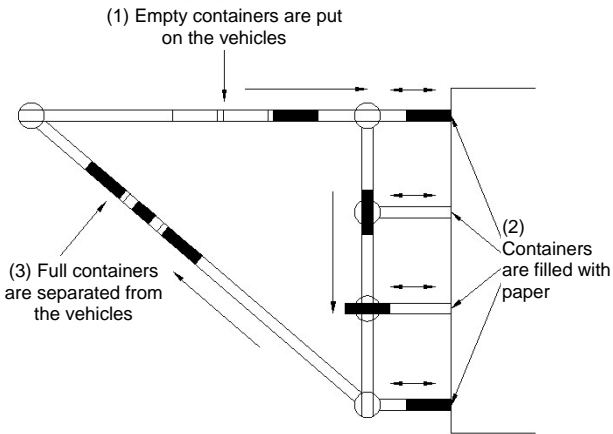


Figure 22. System layout

#### 4.2 Components description

The components were designed to be as simple and robust as possible. Figure 23 shows the basic design of a rail carrier. Four twistlocks make a safe connection to the corner fittings of a container. The steel frame rests on four wheel boxes. Two of them are connected to a gear wheel drive. Distance control to the neighbouring vehicle is performed by laser technology.

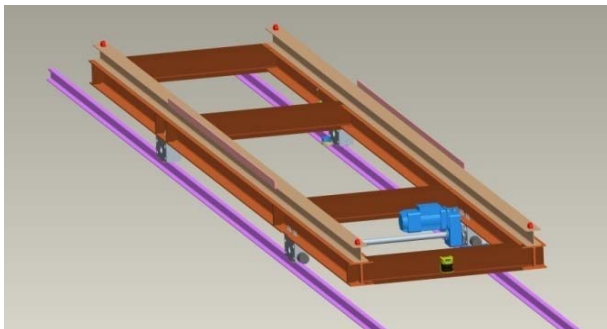


Figure 23. Rail guided carrier

##### Specification of vehicles:

- Total length  $L = 12200$  mm;
- Axis distance  $L_r = 6000$  mm;
- Acceleration  $a = 0.2$  m/s<sup>2</sup>;
- Velocity  $v_{\max} = 63$  m/min;
- Power  $P = 5.5$  kW.

Figure 24 shows the basic design of the turntables to change the direction of the container carriers. Two rails on top of a steel frame with a length of 7 meters provide the necessary space for one carrier. The steel frame is centred with a pivot and rests on four wheel boxes, each driven by an individual gear drive. The wheels rest on a circular base frame with rails.

##### Specification of turntables:

- Length  $L = 7000$  mm;
- Acceleration  $a = 0.2$  m/s<sup>2</sup>;
- Velocity  $v_{\max} = 50$  m/min;
- Power  $P = 4 \times 1.5$  kW;
- 90° cycle time  $t_{\text{turn}} = 15$  s.

Redundant safety components are installed to permit safe automated operation. The complete transportation area is fenced in. Whenever a door in the fence is

opened the entire power supply is shut off and the vehicles stop. As sections 1 and 3 are partially unfenced, ultrasonic sensors are connected to the vehicles. Within a safety distance of one metre the vehicles stop, and only resume their operation automatically when the obstacle is removed.

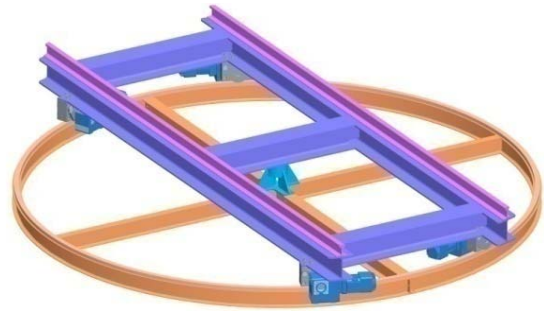


Figure 24. Turntable

#### 4.3 Queuing model

The transportation system according to Figure 22 is modelled as a closed queuing network with a M/M/S/N-system (Fig. 25).

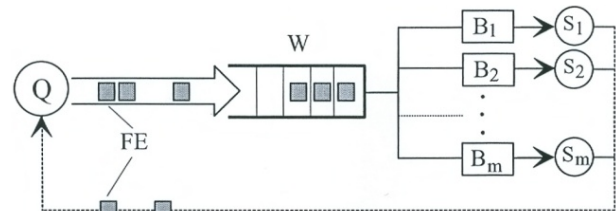


Figure 25. Closed queuing model (M/M/S/N-system)

The description parameters follow Kendall's notation with M describing Markov processes for the arrival and service processes, S = 4 docks as the number of parallel servers and N as the number of vehicles operating in the closed system with a service rate of two containers per hour at each server (dock). The arrival rate  $\lambda$  is calculated from the transport time after leaving the dock stations:

$$t_{\text{out}} = \frac{L_{\text{out}}}{v} + 7 \frac{v}{a} + 2t_d + t_{\text{fo}} + t_{\text{cr}} = 905 \text{ s.} \quad (16)$$

The first two terms account for the travelling time of the vehicles on the rails,  $t_d = 10$  s rotation time of a turntable, and  $t_{\text{fo}} = t_{\text{cr}} = 300$  s, loading time by forklifts  $t_{\text{fo}}$  and unloading time by the container crane  $t_{\text{cr}}$ .

The total time of  $t_{\text{out}} = 905$  results in an arrival rate  $\lambda = 3600/t_{\text{out}} = 3.978$  ct/hr.

From Hillier and Lieberman's equations [6] for closed networks of queues we can calculate the probability of finding n vehicles in the system

$$P_{n1}(n) = \left[ \frac{N!}{(N-n)!n!} \right] \left( \frac{\lambda}{\mu} \right)^n P_0 \quad (17)$$

if  $n = 0 \leq S$ , and

$$P_{n2}(n) = \left[ \frac{N!}{(N-n)!S!S^{n-1}} \right] \left( \frac{\lambda}{\mu} \right)^n P_0 \quad (18)$$

if  $S \leq n = N$ .



The probability of finding zero vehicles in the system is

$$P_0 = \frac{1}{\sum_{n=0}^{S-1} \left[ \frac{N!}{(N-n)!n!} \left( \frac{\lambda}{\mu} \right)^n \right] + \sum_{n=S}^N \left[ \frac{N!}{(N-n)!S!S^{n-1}} \left( \frac{\lambda}{\mu} \right)^n \right]} \quad (19)$$

Finally the number of units waiting in the line is

$$L_q = \sum_{n=S}^N [(n-S)P_{n2}(n)] \quad (20)$$

and where L as number of carriers in the waiting system

$$L = \sum_{n=0}^{S-1} (nP_{n1}(n)) + L_q + S \left( 1 - \sum_{n=0}^{S-1} P_{n1}(n) \right). \quad (21)$$

These equations were evaluated with the number of vehicles varying from  $N = 4$  to 10 and are shown in Figure 26.

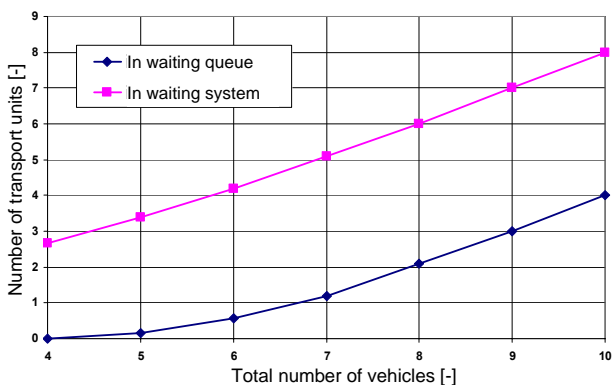


Figure 26. Number of units L and  $L_q$  in waiting system vs. number of vehicles

We see that for  $N = 4, 5$  and 6 vehicles the number of containers in the waiting line before turntable 1 is smaller than one. The result is that one or some of docking stations 1 – 4 are possibly under-utilised. If the number of vehicles exceeds seven we see that the curves of L and  $L_q$  are parallel. It follows that a longer waiting line does not improve system performance. Therefore a maximum of seven vehicles can be assumed to be optimal under the above operating conditions.

#### 4.4 Simulation

In order to validate the results obtained, a simulation study was also conducted. A discrete event simulation software package named Plant Simulation was used to consider effects such as varying the length of the queue or more accurate modelling of resources.

First a triangular rail path with unidirectional traffic was modelled, including the docking stations. Each corner of the triangle and each shunt to the docking stations contained a turntable as a pick and place element. The rail guided vehicles exist as preconfigured resources in Plant Simulation. Only parameters like  $L, v, a$  have to be defined according to the technical specifications (Fig. 27).

Cycle times at the forklift and crane stations were assumed to be constant at five minutes. The average

loading times at the docks were assumed to be 30 minutes with an exponential distribution. Graphical representation on the screen permitted quick control of the model and its animated operation. Comparing the results in Figure 28 to the queuing model shows good compliance of the two models.

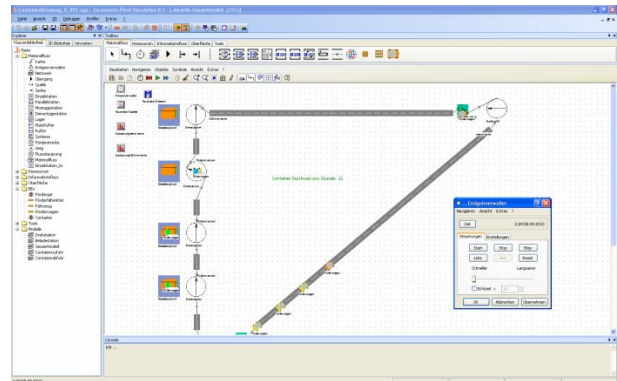


Figure 27. Simulation model

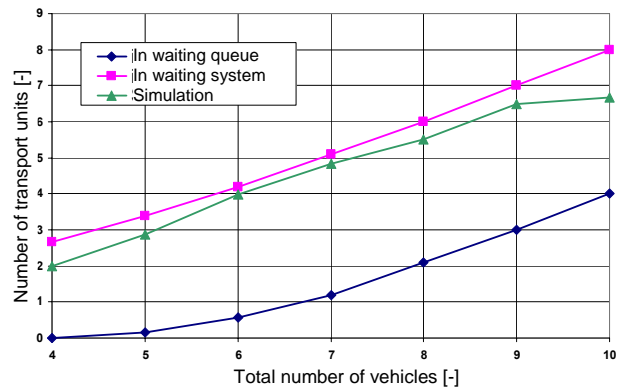


Figure 28. Comparison of simulation and queuing analysis

A throughput diagram in Figure 29 shows simulation results with a maximum of seven vehicles in the system. A further increase in the number of vehicles only increases congestion, but not throughput.

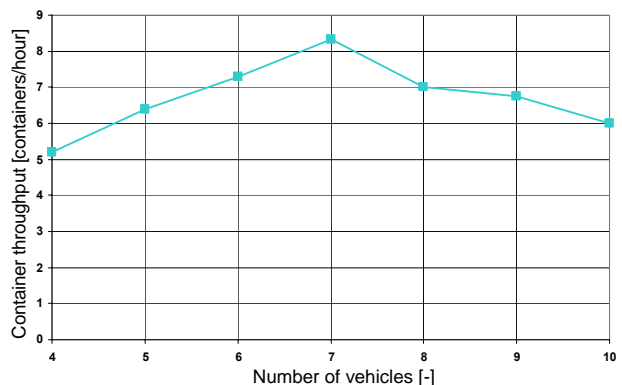


Figure 29. Container throughput vs. number of vehicles

#### 4.5 Summary of case study 3

This case study deals with a novel system for automated container transport. The technical solution is based on a rail system, turntables and rail guided vehicles for the container transport.

The optimum number of vehicles was evaluated using a queuing model and a simulation model. The results were in close agreement.

## 5. CONCLUSION

In this paper three case studies, related to the three levels of technical logistics were presented: components, conveyors and logistics systems. In each

case study at least two of the three potential methodologies (Table 2) were applied. Doing so has the advantage that the results are reliable and that there is a good chance of identifying an optimum solution.

**Table 2. Methods applied on the case studies**

	Analytic calculation	Simulation	Measurement
<b>3. Level: Logistics systems</b> Automated container terminal	Queuing theory	Logistics simulation	Measurement of cycle times
<b>2. Level: Conveyors</b> Friction damper for AS/RS	Calculation of a two mass system	Numerical simulation	Measurement on a test stand
<b>1. Level: Components of material handling</b> Fly-wheel brake	Static calculation	Multi body simulation	Measurement on a test stand

## REFERENCES

- [1] DIN EN 341 Personal Protective Equipment Against Falls from a Height – Descender Devices for Rescue, 2003, (in German).
- [2] Kurth, F. and Scheffler, M.: *Fundamentals of Mechanical Conveying*, VEB Verlag Technik, Berlin, 1976, (in German).
- [3] Kartnig, G. and Landschuetzer, C.: Analytic and experimental investigations on a rescue device, in: *Proceedings of the XVIII International Conference on Material Handling, Constructions and Logistics – MHCL'06*, 19-20.10.2006, Belgrade, Serbia, pp. 227-234.
- [4] Hornhofer, F., Kartnig, G. and Oser, J.: Optimisation of friction dampers for storage machines, *DHF Intralogistik*, Vol. 10, pp. 70-74, 1997, (in German).
- [5] Kartnig, G., Oser, J.: System design and operation of a small size container terminal, in: *Proceedings of the 20th Annual Conference of the Production and Operations Management Society – POMS 2009*, 01-04.05.2009, Orlando, USA.
- [6] Hillier, F.S. and Lieberman, G.J.: *Introduction to Operations Research*, McGraw-Hill, New York, 2005.

## СТРУКТУРА И МЕТОДЕ У ОБЛАСТИ ИНЖЕЊЕРСКЕ ЛОГИСТИКЕ

Георг Картниг

Област инжењерске логистике се бави руковањем материјала на три нивоа: 1. компоненте, 2. транспортери и 3. логистички системи. Субјекти сваког од три нивоа могу се истраживати помоћу три методе: 1. аналитичким приступом, 2. симулацијом и 3. испитивањем. У раду су приказане три студије стања које описују како се проблеми у области инжењерске логистике могу решавати применом садашњих технологија.